Master's Thesis of Engineering

Uncertainty and Sensitivity Analyses of Dynamic Solar Heat Gain Coefficient for Window System with External Venetian Blind

외부 블라인드가 설치된 창호 시스템의 동적 SHGC의 불확실성 및 민감도 분석

August 2023

Department of Architecture and Architectural Engineering
College of Engineering
Seoul National University

JeongYun Lee

Uncertainty and Sensitivity Analyses of Dynamic Solar Heat Gain Coefficient for Window System with External Venetian Blind

Advised by Prof. Cheol-Soo Park

Submitting a master's thesis of Engineering

August 2023

Department of Architecture and Architectural Engineering
College of Engineering
Seoul National University

JeongYun Lee

Confirming the master's thesis written by
JeongYun Lee

August 2023

Chair	Myoung-Souk Yeo	(Seal)
Vice Chair	Cheol-Soo Park	(Seal)
Examiner	Sun Sook Kim	(Seal)

Abstract

The thermal properties of the window system have been treated in a deterministic fashion and physically calculated under static boundary conditions. However, the stochastic variation of thermal performance is known to be caused by environmental conditions as well as blind slat angles. This study investigates the stochastic characteristics of SHGC of a double-glazing system with an external Venetian blind. A virtual environment was constructed to simulate dynamic thermal behavior. It primarily relies on the pyWinCalc program, which is a stand-alone tool. Design, control, and environmental variables are parameterized to account for the system's different configurations and operational strategies under various conditions.

By sensitivity analysis, the influence of each environmental variable on SHGC was determined, and it was found that its ranking varied depending on the slat control angle. Uncertainty analysis revealed that the uncertainty in SHGC is significant and influenced by environmental variables and slat angles. The degree of variations and distribution of SHGC depending on the slat control angles were analyzed by considering seasonal differences and diurnal variations.

This study suggests the importance of a stochastic assessment of the thermal performance of window systems and the implementation of dynamic control for external Venetian blinds. It also can contribute to developing guidelines for manual slat control by occupants.

Keyword : External Venetian Blind, Solar Heat Gain Coefficient, Uncertainty Analysis, Sensitivity Analysis, Performance Gap

Student Number : 2021-26763

Table of Contents

List of Figures

List of Tables

Chapter 1. Introduction

1.1 Problem Statement and Objectives of Study

The transparent building envelope has been widely used because it can provide thermal and visual comfort to occupants by introducing solar radiation. However, it could also transmit unwanted solar energy into the indoor space and cause severe visual discomfort in an over-daylit environment. Furthermore, the cooling and heating load can increase due to its lower insulation performance, significantly impacting building energy consumption. Hence, indoor and outdoor shading devices are generally used to control the amount of absorbed and transmitted solar energy through the transparent envelope. The shading effect of a transparent envelope with shading devices is necessary for the design phase to install appropriate shading devices depending on the building profile, schedule, and climate and to utilize them optimally in the operating phase. The thermal performance of the system is mainly expressed by two factors, which are the overall heat transfer coefficient (U-value) and solar heat gain coefficient (ASHRAE, 2019). Of these, SHGC is defined as the ratio of the solar heat gain through the window and the solar radiation incident on the window. Since SHGC has optical characteristics reflecting solar transmittance and absorptance, it varies depending on the solar incidence angle, and it is influenced by many factors such as slat angles, material properties (reflectance and absorptance) of slats, and environmental boundary conditions (direct and diffuse solar radiation, and wind velocity).

The current measurement of the SHGC for window systems involves conducting experiments in a controlled physical chamber. Thus, international standards have been developed to define boundary conditions in a deterministic fashion. As shown in Figure 1.1, in existing international standards related to SHGC, such as KS L 9107 (2014), ISO 15099 (2003), and NFRC 200 (2020), the indoor/outdoor boundary conditions and amount of direct irradiance at a normal angle are defined as static values. The chamber should maintain these conditions in a steady state, and the transmitted heat is measured to determine the static SHGC. The derived value is used as a key input parameter in most building energy analysis tools (e.g., ISO 13790, EnergyPlus).

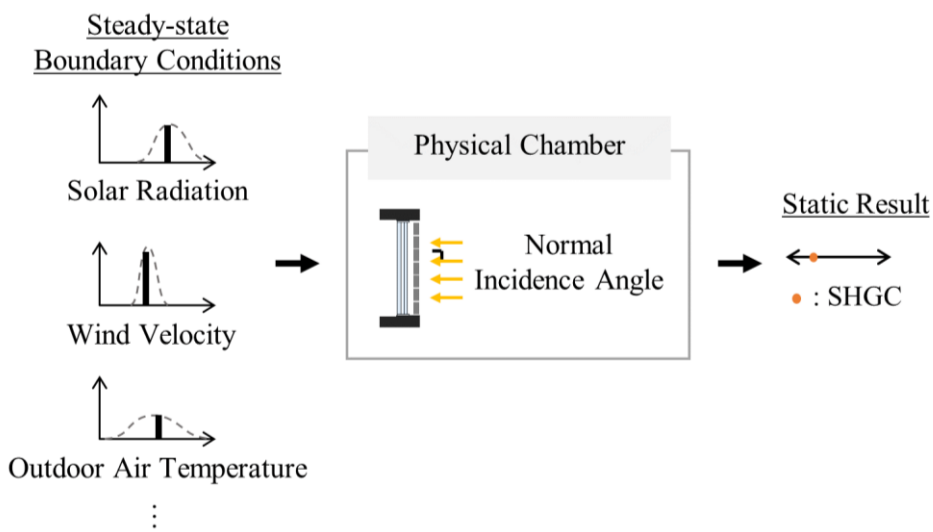

Figure 1.1 Deterministic approach

However, the indoor and outdoor environments of an actual building have stochastic characteristics, and it has been acknowledged that many types of uncertainties exist in building energy modeling (de Wit and Augenbroe, 2002; Hopfe, 2009). In addition, the existing methods do not consider the effect of the solar incidence angle and diffuse solar radiation and the control performance of adjustable shading devices. Thus the result of the deterministic approach may not represent the actual thermal behavior of the window system under a constantly varying environment. It causes a performance gap between dynamic simulation predictions and reality (de Wilde, 2014) and may not meet the energy savings expected in the design phase. Nevertheless, no research has been conducted to quantify the change in the flow of solar heat energy and the system's thermal performance, according to control methods and dynamic environmental conditions in window systems with external Venetian blinds.

Hence, this study was conducted to investigate the stochastic characteristic of the SHGC through continuous simulations. As shown in Figure 1.2, as a substitute for the physical chamber used in deterministic experiments, a virtual environment called 'Virtual Testbed' was constructed to simulate the system's behavior under various environmental, design, and control variables. Through the virtual testbed, the uncertainty in the SHGC of the window system was quantified, and the stochastic characteristic of the system's thermal performance was captured.

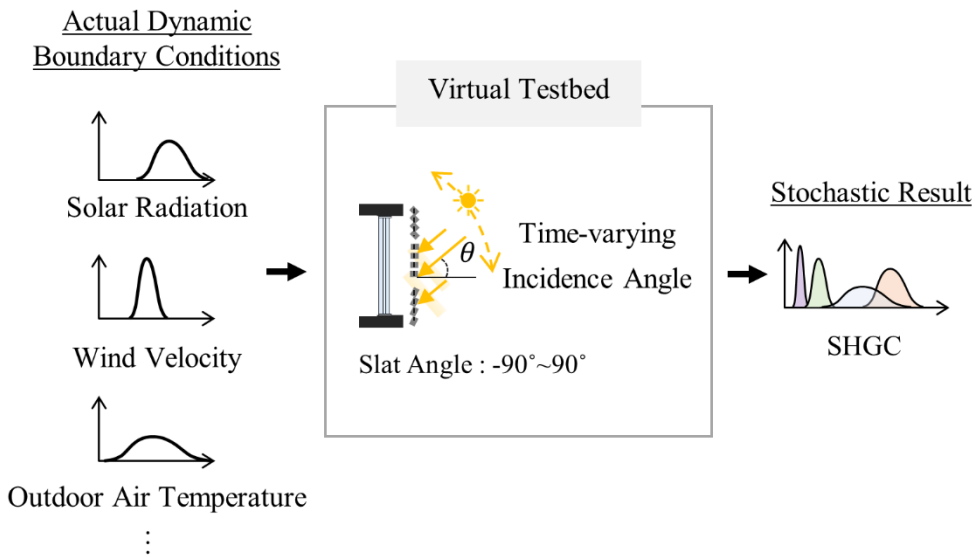

Figure 1.2 Stochastic approach

In previous research on optimal control of adjustable shading devices, a dynamic simulation tool was employed to develop a building energy simulation model. The objective was to derive the optimal control variable, specifically the slat angle of the blinds, by utilizing a cost function related to cooling and heating energy consumption (Kim & Park, 2010; Kim & Park, 2012; May-Ostendorp et al., 2012; Huchuk et al., 2016). Due to the structural characteristics of dynamic simulation tools, this approach is challenging to interpret the dynamic characteristics of the building and the dynamic behavior of external Venetian blinds separately. In this study, an external blind model is independently designed to perform sensitivity and uncertainty analyses. By utilizing a stand-alone tool (White-Box model), and not resorting to dynamic whole-building simulation tools, there is an advantage in the process of derivation of the thermal performance of the shading system (Figure 1.3). Unlike other dynamic building energy simulation tools (Black-Box Model), which can derive the thermal performance of the system through an inverse calculation process

for energy values obtained from the output, it independently analyzes the thermal performance of the shading system without relying on the building model.

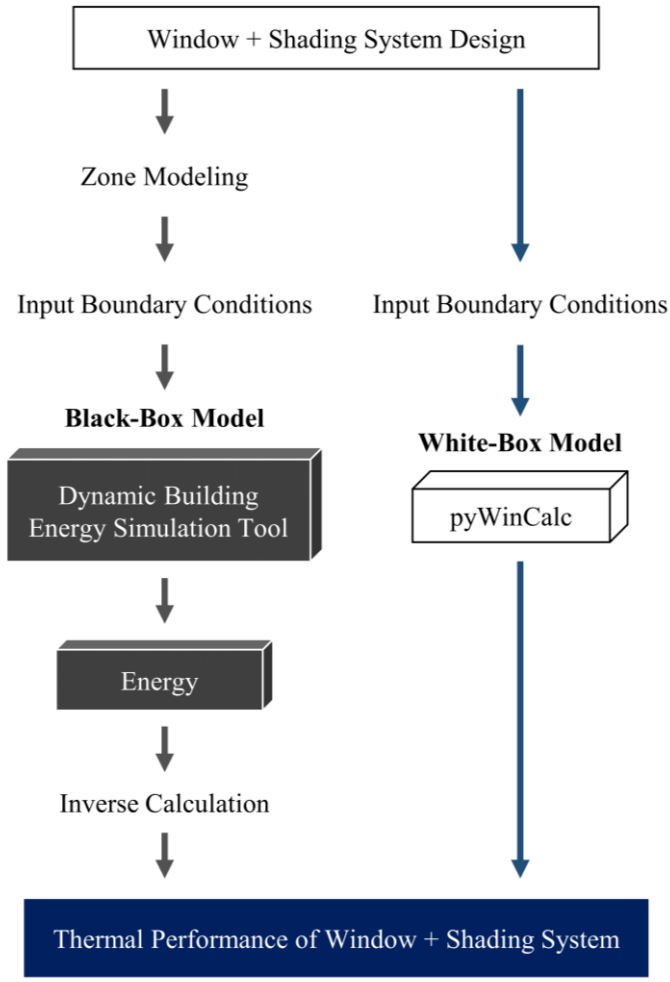

Figure 1.3 Comparison in the derivation of thermal performance between two methods

1.2 Organization of Thesis

In the previous chapter, the necessity of a stochastic approach in the calculation of SHGC of a window system is described and simulation process involving a stand-alone tool is explained. The organization of the thesis is as follows:

- Chapter 2 discusses the necessity of this study through a literature review of the impact of SHGC on building energy and existing international deterministic standards to measure SHGC. Also, it provides a background on sensitivity and uncertainty analyses.
- Chapter 3 presents the details about methodology applied in the simulation. A virtual testbed based on pyWinCalc system is described and a novel approach of SHGC calculation is introduced.
- Chapter 4 describes a simple window system with an external Venetian blind designed in the pyWinCalc system for continuous simulation.
- Chapter 5 presents the results of the point-in-time simulation, seasonal simulation, and diurnal simulation. It is described in figures and tables with detailed values.
- Chapter 6 completes the thesis by providing a summary and conclusion of the study.

Chapter 2. Literature Review

Many studies analyzed the impact of SHGC on the window systems on building energy consumption. Park and Park (2010) analyzed the impacts of SHGCs of windows on the energy use of houses through energy simulation, and confirmed the necessity of proper SHGC value by region. Choi and Chang (2013) analyzed heating and cooling load associated with window performance indicators, orientation, and latitude on the building energy consumption with systematically designed simulations in different target regions. They found that performance indicators and orientation achieve a dramatic reduction in energy consumption.

2.1 Measurement of SHGC

SHGC is widely used as an indicator for evaluating the thermal performance of window systems. Generally, the SHGC of the window system is calculated through physical experiments. International standards have been developed to define boundary conditions in a deterministic fashion, because in order to quantify dynamic variation in SHGC, an infinite number of tests should be conducted. National Fenestration Rating Council (NFRC) provides ANSI/NFRC 200 (2020) for SHGC calculations in the United States. In South Korea, SHGC experiments of the window system are conducted according to KS L 9107 (2014) set by Korean Industrial Standard (KS). SHGC of window systems with shading devices is evaluated by measurement test method by the solar simulator, and the measuring device consists of a chamber integrated with a solar simulator and measures the acquisition of heat using the calorimetry method in the static condition, as Table 2.1 shows. Even though there is a difference in boundary conditions between international standards, they all

adopt a deterministic fashion. This static SHGC value obtained from the experiments has been used as input parameters in most building simulation tools.

Table 2.1 Deterministic boundary conditions for calculation of SHGC

Standard		Temperature [℃]		Surface Heat Transfer Rate [W/(m^2·K)]		Irradiance [W/m^2]
		Exterior	Interior	Exterior	Interior	
KS L 9107	Winter	0 (±1)	20 (±1)	20 (±1)	9 (±1)	300
	Summer	30 (±1)	25 (±1)	15 (±1)	9 (±1)	500

2.2 Sensitivity and Uncertainty Analyses

Sensitivity and uncertainty analyses are necessary to quantify the level of uncertainty in the results of the simulation and to analyze the influence of each input variable on the results (Hopfe & Hensen, 2011). The Sobol method, one of the global sensitivity methods, was used because it can effectively quantify fluctuations in the output for the entire input parameters that were sampled simultaneously (Sobol, 1993; Mara & Tarantola, 2008). The Sobol method derives the sensitivity of input parameters by dividing the conditional variance ($V_{X_i}(E_{X_{\sim i}}(Y|X_i))$) for an input variable (X_i) with respect to the output variable (Y) by the total variance ($V(Y)$) of the output variable as shown in Equation 2.1. The sensitivity ranking of input variables was obtained using the first-order sensitivity index (S_i). It is the stand-alone sensitivity of the i^{th} input variable, representing the independent sensitivity of each input variable in the state of the interaction with other variables being removed. The second-order sensitivity index (S_{ij}) refers to the effect of the interaction effect between the target

input variable and other input variables, and the n^{th} sensitivity index refers to the effect of interaction between the input variable and *(n-1)* other variables. The sum of the sensitivity indices of all input variables except the overlapped effect by the interaction corresponds to 1.0 (Equation 2.2). The Sobol method can quantify the importance of all input variables, and the first-order sensitivity index (S_i) of each variable is expressed as a number between 0.0-1.0, and the closer it becomes to 1.0, the greater the influence on the output variables.

$$S_i = \frac{V_{X_i}(E_{X_{\sim i}}(Y|X_i))}{V(Y)} \tag{2.1}$$

$$\sum_i S_i + \sum_i \sum_{j>i} S_{ij} + \sum_i \sum_{j>i} \sum_{k>j} S_{ijk} + \cdots + \mathrm{S}_{123\ldots\mathrm{z}} = 1 \tag{2.2}$$

Latin Hypercube Sampling (LHS) was used for uncertainty analysis to examine the variation of the output. LHS is an improvement over simple random sampling and stratified sampling, addressing the issue of sample bias. It allows for generating samples that ensure uniformity within the probability distribution. It divides the parameter space into bins of equal probability with the goal of attaining a more even distribution of sample points in the parameter space, which would be possible with pure random sampling (McKay, 2000).

Chapter 3. Methodology

3.1 Virtual Testbed

A virtual testbed was constructed to parameterize variables in Python to perform simulations under various environmental conditions continuously. It primarily relies on the 'pyWinCalc' program (Kohler et al., 2019), a Python package of WINDOW Engine (LBNL, 2016) developed by Lawrence Berkeley National Laboratory. It has the advantage of including a calculation scheme for determining the angular dependence of the glazing system's optical properties. The materials' thermal and optical characteristic information in the International Glazing and Shading Database (LBNL, 2022) is freely utilized. Design variables, such as the size of the window and the length, spacing, and control variables, such as the slat angle of the blind, are parameterized to account for different configurations and operational strategies of the system. As shown in Figure 3.1, it is possible to incorporate scalable conditions that vary based on building type, climate zone, and other factors into a parameterized system to account for different conditions and scenarios, and the thermal performance of the window system is calculated as output.

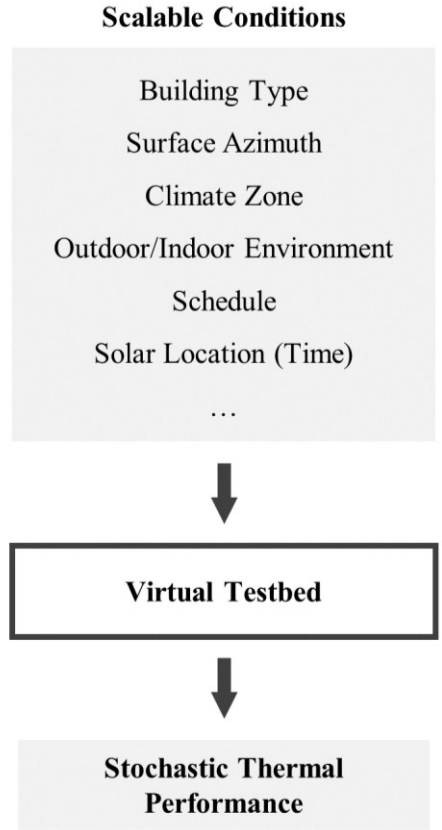

Figure 3.1 Scheme of simulation

3.2 SHGC Calculation

Solar Heat Gain Coefficient (SHGC) is a function of the solar transmittance, the solar absorptance, and the inward-flowing fraction of thermal energy (Equation 3.1; Curcija et al., 2018). SHGC is widely used to evaluate the thermal performance of window systems and can be utilized for the quantitative performance assessment of shading devices. It is also defined as the ratio of the solar heat gain through the window and the solar radiation incident on the window, reflecting all solar heat transfer effects introduced into the indoor space. It varies depending on environmental conditions and the angle of incidence of sunlight, as it reflects optical characteristics such as transmittance and absorptance. Thus, SHGC is an indicator that is influenced by many factors, such as environmental boundary conditions, optimal material properties of the system, and slat control angles.

$$SHGC = T_{sol} + N * A_{sol} \tag{3.1}$$

*T_{sol} : total solar transmittance of a window

*A_{sol} : total solar absorptance of a window

*N : number of the inward flowing fraction

In actual environments, the effect of both direct and diffuse radiation exists, and thus it is necessary to evaluate the impact of both types of solar radiation. The direct and diffuse components of the incident solar radiation have to be separated, and the total amount of solar heat introduced indoors (Q_{solar}) can be obtained by multiplying the direct solar radiation (I_{dir}) and diffuse solar radiation (I_{dif}) by each solar heat acquisition coefficient (Equation 3.2; Kreider et al., 2016). As a result, the solar heat acquisition coefficient ($SHGC_{glo}$) to the amount of global solar radiation (I_{glo}) can be expressed as a ratio of the amount of solar radiation (Q_{solar}) introduced into the room to the amount of solar radiation reaching the outer surface of the window (Equation 3.3).

$$Q_{solar} = \mathrm{SHGC_{dir}}\ I_{dir} + \mathrm{SHGC_{dif}}\ I_{dif} \tag{3.2}$$

$$\mathrm{SHGC_{glo}} = \frac{Q_{solar}}{I_{glo}} = \frac{SHGC_{dir}\ I_{dir} + SHGC_{dif}\ I_{dif}}{I_{dir} + I_{dif}} \tag{3.3}$$

The amount of direct solar radiation to reach the window (I_{dir}) can be calculated based on direct normal radiation (I_{DNI}). It is calculated by multiplying by the cosine value of the solar incidence angle on the plane(θ_i) (Equation 3.4). Since the position of the sun varies throughout the day, as shown in Figure 3.2, in pyWinCalc system, the direction of direct beam radiation viewed from within the shading system is defined using relative altitude angle (θ) and azimuth angle (φ) (Figure 3.3). Therefore, SHGC for direct radiation ($SHGC_{dir}$) can be derived by inputting the two solar coordinates into the pyWinCalc system (Equation 3.5).

$$I_{dir} = I_{DNI}\ cos(\theta_i) \tag{3.4}$$

$$\mathrm{SHGC_{dir}} = P(\theta, \varphi) \tag{3.5}$$

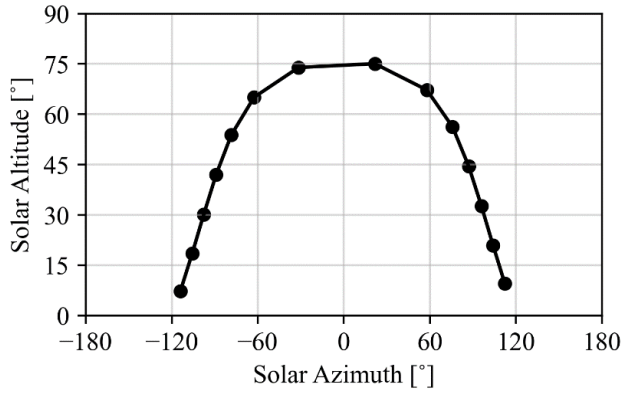

Figure 3.2 Cylindrical projection sun-path diagram for 21 June

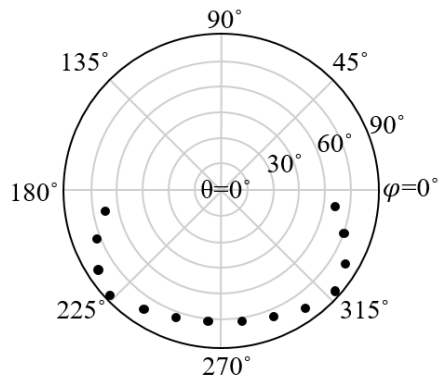

Figure 3.3 Polar projection sun-path diagram in pyWinCalc system for 21 June

In order to calculate the effect of diffuse solar radiation, diffuse properties can be determined by integrating properties at over all directions. It is based on the principle that energy flow through the glazing should equal the sum of individual energy flows caused by incident radiation from each direction. The spectral dependence is assumed to be the same as for beam solar radiation and both sky and ground radiation are assumed to be ideally diffuse, a diffuse property (X_D) can be generally defined as Equation 3.6 (ASHARE, 2019). In BSDF, every patch is defined through two angles (θ, φ) given in the hemispherical coordinate system. As shown in Figure 3.4, this infinitely small patch (dA) will have a surface area (Equation 3.7). The solid angle of the patch is then equal to Equation 3.8. The value of $SHGC_{dif}$ is calculated from the integral sum of $SHGC_{dir}$ over all incident angles as in Equation 3.9, and finally summarized as Equation 3.10.

$$X_D = \frac{\iint X(\theta) cos\theta d\omega}{\iint cos\theta d\omega} \tag{3.6}$$

$$dA = d\theta \cdot r \cdot sin(\theta) \cdot d\varphi \cdot r \tag{3.7}$$

$$d\omega = \frac{dA}{A} = \frac{d\theta \cdot r^2 \cdot sin(\theta) \cdot d\varphi}{2\pi r^2} = \frac{1}{2\pi} sin\,(\theta) d\theta d\varphi \tag{3.8}$$

$$\frac{\int SHGC_{dir} cos(\theta) d\omega}{\int \cos(\theta) d\omega} = \frac{\int_0^{\pi} \int_0^{\frac{\pi}{2}} P(\theta,\varphi) \frac{1}{2\pi} cos(\theta) sin(\theta) d\theta d\varphi}{\int_0^{\pi} \int_0^{\frac{\pi}{2}} \frac{1}{2\pi} sin(\theta) d\theta d\varphi} = \frac{\int_0^{\frac{\pi}{2}} \int_0^{\pi} \frac{1}{2\pi} cos(\theta)\, sin(\theta) d\theta P(\theta,\varphi) d\varphi}{\frac{1}{2}} \tag{3.9}$$

$$\mathrm{SHGC_{dif}} = \; 2 \int_0^{\frac{\pi}{2}} \mathrm{SHGC_{dir}} cos(\theta) sin(\theta) d\theta \tag{3.10}$$

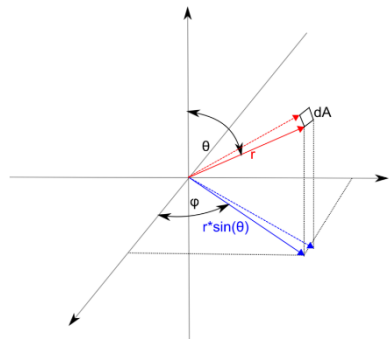

Figure 3.4 Spherical coordinates and patch (Curcija C. et al. , 2018)

Chapter 4. Target System

For this study, a general double-layer window system was selected for analysis. It is assumed that the system is located in Seoul, South Korea, and south-faced. It consists of two layers of interior and exterior 6mm clear glazing with a 12mm air gap and external Venetian blinds. The width and height of glazing are 1,000mm (Table 4.1), and the effect of the frame is not considered for an intuitive interpretation of simulation results. The blind slats are opaque white with a solar reflectance of 0.64, solar transmittance of 0.0, and infrared emittance of 0.80. The slat's width and vertical spacing are 50mm. Assuming a range of -90˚ to +90˚, the blind slats are represented with an angle of 0° when they are in a horizontal position, with upward-facing angles expressed as negative and downward-facing angles expressed as positive (Figure 4.1). In order to conduct simulation, the slat angle of the blind was discretized at intervals of either 10° or 20° and analyzed by each slat angle.

Table 4.1 Experimental conditions and properties of target window system

Glazing properties	Width	1,000 mm
	Height	1,000 mm
	Composition	6 mm clear glazing + 12 mm air + 6 mm clear glazing
Slat properties	Width	50 mm
	Spacing	50 mm
	Thickness	0.2 mm
	Slat Angle	-90˚, -80˚, -70˚...70˚, 80˚, 90˚ (10˚ or 20˚ intervals)
	Solar reflectance	0.64
	Infrared emittance	0.80

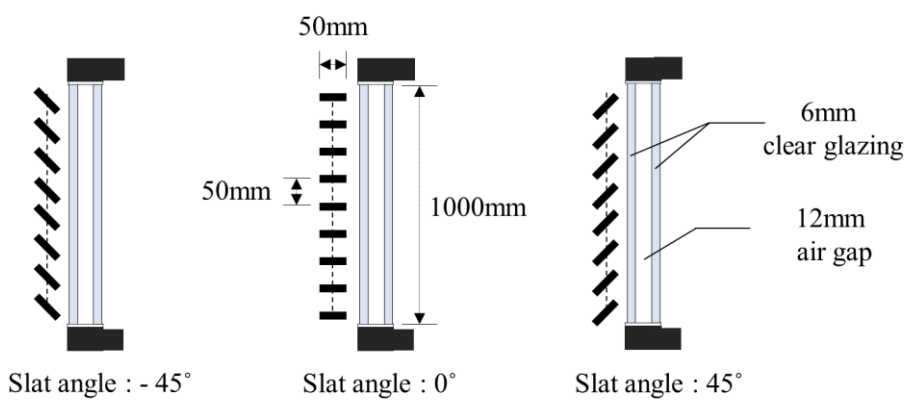

Figure 4.1 Target window system with external blind slats

Chapter 5. Simulation Results

5.1 Point-in-time Analysis

For sensitivity and uncertainty analyses, a point-in-time analysis was conducted at a selected particular time point. June 21st at 1 pm, with a solar altitude of 75.1˚ and azimuth of 21.6˚, is the time point selected when a sufficient amount of solar radiation and variation in weather conditions are secured. As aforementioned, the window system is assumed to be located in Seoul, South Korea, with a longitude of 126°E and a latitude of 37.5°N.

5.1.1 Sensitivity Analysis

Uncertainty analysis and sensitivity analyses are performed based on Monte Carlo sampling. First, the following environmental variables were used: outdoor air temperature, indoor air temperature, direct and diffuse solar radiation, outdoor wind velocity, and outdoor wind direction. Then, the range of variables was derived, as shown in Table 5.1, by referring to standard weather data of Seoul. Then, using the Saltelli sampling scheme (Saltelli et al., 2008), 1,024($= 2^{10}$) samples were generated, and a total of 14336 ($= 2^{10} \times (2 \times 6 + 2)$) environmental sample combinations were generated (Equation 5.1) and inputted into the virtual testbed, resulting in the calculated output values ($SHGC_{dir}$, $SHGC_{dif}$, $SHGC_{glo}$). Subsequently, for each slat angle discretized at 20° intervals, the SHGC distribution was derived.

$$N \times (2D + 2) \tag{5.1}$$

$N =$ number of samples (2^{10})

$D =$ number of parameters (6)

Table 5.1 Sampling range of environmental variables

Environmental Variable	Min	Max
Outdoor Air Temperature	13.1℃	36.2℃
Indoor Air Temperature	24.0℃	28.0℃
Direct Solar Radiation	100W/m^2	810W/m^2
Diffuse Solar Radiation	154W/m^2	489W/m^2
Outdoor Wind Velocity	0.7m/s	7.89m/s
Outdoor Wind Direction	0°	360°

The Sobol method was employed for $SHGC_{glo}$, which is one of the global sensitivity analysis methods which explores the entire input variable space, which requires a large number of simulation iterations. It provides the sensitivity indices of input parameters using the conditional variance of the output.

Among the environmental variables, direct solar radiation (I_{dir}), diffuse solar radiation (I_{dif}), and wind velocity were found to account for more than 90% of the total uncertainty. Table 5.2 represents first-order sensitivity indices of six variables according to nine different slat angles. The first-order sensitivity index of direct solar radiation (mean: 0.595) was higher than that of diffuse solar radiation (mean: 0.267) across all slat angles.

It appeared challenging to find the dynamic characteristics of $SHGC_{glo}$ based on outdoor wind velocity. However, when the slats rotate upward (positive direction), there is a decrease in the absolute amount of solar radiation transmitted through the transparent envelope, resulting in an increase in the influence of wind velocity

(maximum: 0.44) and a decrease in solar radiation. Nevertheless, it is crucial to note that even with notable first-order sensitivity indices, the actual impact on SHGC may not be significantly pronounced. This is because the overall uncertainty, indicated by the total difference of SHGC(△SHGC), decreased as the slats rotated upward.

Table 5.2 First-order sensitivity index from Sobol

Slat Angle	-80 °	-60 °	-40 °	-20 °	0 °	20 °	40 °	60 °	80 °
Direct Solar Radiation	0.69	0.68	0.68	0.68	0.67	0.65	0.60	0.48	0.32
Diffuse Solar Radiation	0.30	0.30	0.30	0.30	0.29	0.28	0.26	0.22	0.15
Wind Velocity	0.00	0.01	0.01	0.01	0.01	0.04	0.11	0.25	0.44
Outdoor Air Temperature	0.00	0.00	0.00	0.00	0.00	0.00	0.00	0.00	0.01
Indoor Air Temperature	0.00	0.00	0.00	0.00	0.00	0.00	0.00	0.00	0.00
Wind Direction	0.00	0.00	0.00	0.00	0.00	0.00	0.00	0.00	0.00
△SHGC	0.13	0.09	0.17	0.15	0.09	0.05	0.03	0.02	0.01

5.1.2 Uncertainty Analysis

Figure 5.1 illustrates the variations of $SHGC_{dir}$ and $SHGC_{dif}$ at nine different slat angles across 14,336 sample combinations. While $SHGC_{dir}$ exhibits a wide range of values, $SHGC_{dif}$ is represented with relatively small uncertainty. As the slats rotate downward, the values of $SHGC_{dir}$ tend to increase and reach a peak value of 0.50 at -60°, subsequently decreasing as the slat rotates upward. This can be attributed to the increased surface area of the shading device exposed to solar radiation as the slat angle approaches the solar altitude angle (75.1°), allowing more solar radiation to pass through the slats and reach the glazing. However, it is noteworthy that despite the fact that the slat angle of -80° is closer to the solar altitude angle, the $SHGC_{dir}$ is smaller compared to -40° due to the slats having a smaller spacing and thus a smaller opening area. The largest uncertainty of $SHGC_{dir}$ is observed at -40°, with a range of 0.14, indicating that the impact of environmental variables can lead to an uncertainty of up to 0.14. On the other hand, as the slats rotate in the positive direction from the horizontal position, both the maximum and minimum values of $SHGC_{dir}$ decrease, resulting in a reduction of the uncertainty range by up to 0.02.

It is observed that the average value of $SHGC_{dif}$ ranges from 0.05 to 0.5 depending on the slat angle. However, the magnitude of uncertainty attributed to environmental variables remains small, equal to or less than 0.01 for all slat angles. This is primarily due to the calculation process of $SHGC_{dif}$, which involves integrating the product of $SHGC_{dir}$ values obtained for each incident angle(θ) multiplied by $\cos(\theta)\sin(\theta)$. As a result, the uncertainty of $SHGC_{dir}$ is reduced by a factor of $\cos(\theta)\sin(\theta)$, leading to a smaller uncertainty for $SHGC_{dif}$. The peak value of $SHGC_{dif}$ occurs at a slat angle of -40° reaching 0.57, which is higher than the values observed at -60° and 80°.

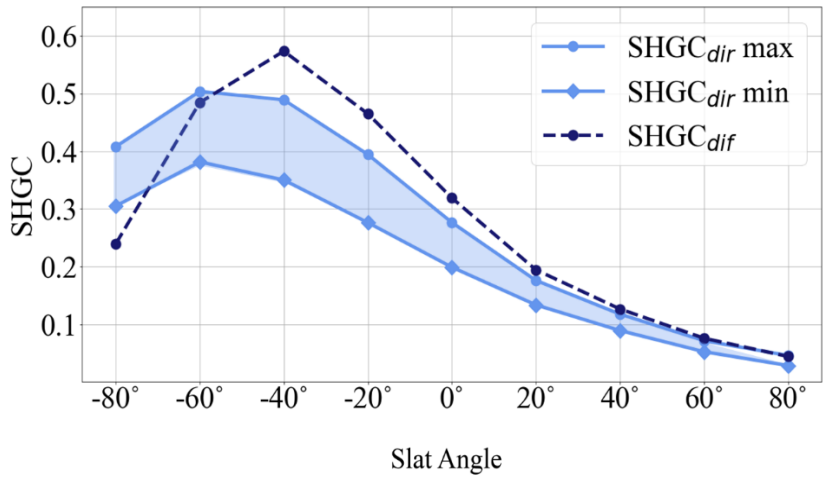

Figure 5.1 $SHGC_{dir}$ and $SHGC_{dif}$ at nine different slat angles

Meanwhile, in the case of the same double-glazing system without any external shading device, the average $SHGC_{dir}$ varied between 0.03 and 0.73 depending on environmental factors. In addition, $SHGC_{dif}$ was found to be smaller than $SHGC_{dir}$ at 0.64, and the deviation also remained constant below 0.01. Under identical environmental conditions, the installation of external Venetian blinds resulted in a decrease in $SHGC_{dir}$ by 0.22-0.71 and $SHGC_{dif}$ by 0.07-0.59 compared to the case without the shading device.

$SHGC_{glo}$ was calculated through Equation 3.3, with $SHGC_{dir}$ and $SHGC_{dif}$ values obtained through simulations. It was shown to follow different normal distributions at each slat angle. The distribution of $SHGC_{glo}$ exhibits a normal distribution pattern for each slat angle. Specifically, when considering the cases of slat angles at 0° and -80°, although the mean values of the distributions are similar, there is a difference in terms of variance (Figure 5.2).

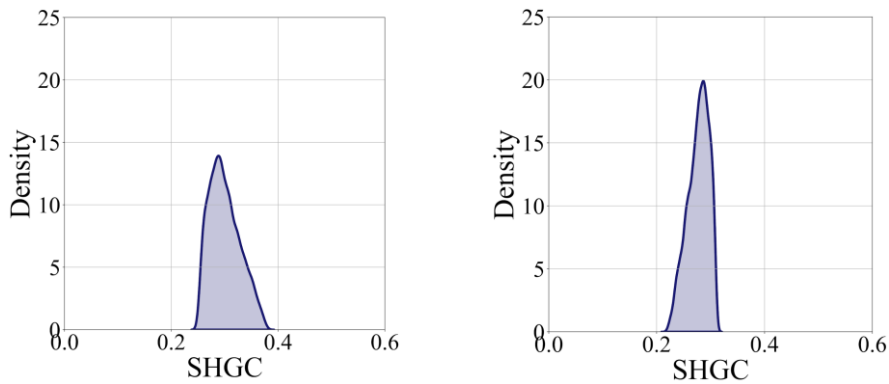

(a) Slat angle at -80° (b) Slat angle at 0°

Figure 5.2 Distribution of $SHGC_{glo}$ at two different slat angles

Figure 5.3 depicts the distributions $SHGC_{glo}$ for each slat angle under varying environmental conditions. It is evident that as the slats rotate upward, both the mean and standard deviation decrease. On the other hand, when the slats are in a horizontal position (0°) or rotated downwards, relatively larger variations in the distribution can be observed. This implies that even for the same slat angle, significant differences can occur depending on environmental variables such as solar radiation, outdoor temperature, and wind velocity. Furthermore, under identical environmental conditions, $SHGC_{glo}$ varied from a minimum of 0.372 (Case 1 in Table 5.3) to a maximum of 0.514 (Case 2 in Table 5.3), depending on the slat control angle.

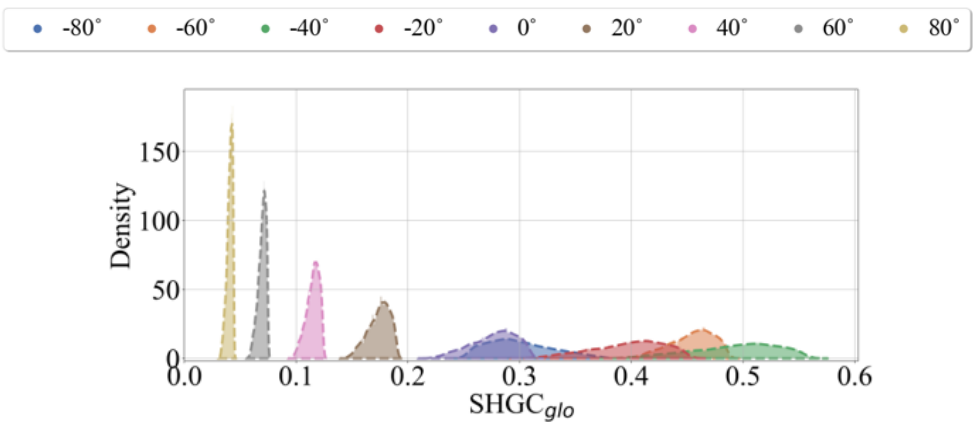

Figure 5.3 Distribution of $SHGC_{glo}$ according to nine different slat angles

Table 5.3 Max and min $SHGC_{glo}$ depending on environmental conditions

		Case 1	Case 2
Difference in $SHGC_{glo}$		0.372 = 0.407-0.035	0.514 = 0.557-0.043
Outdoor Air Temperature		22.8℃	27.5℃
Indoor Air Temperature		27.2℃	26.4℃
Direct Solar Radiation		830.7W/m^2	100.4W/m^2
Diffuse Solar Radiation		154.8W/m^2	474.1W/m^2
Outdoor Wind Velocity		4.0m/s	4.1m/s
Outdoor Wind Direction		7.9°	128.5°
Maximum	Slat Angle	-60°	-40°
	$SHGC_{glo}$	0.407	0.557
Minimum	Slat Angle	80°	80°
	$SHGC_{glo}$	0.035	0.043

Figure 5.4 depicts a variation of $SHGC_{glo}$ according to global solar radiation by slat angles. Additionally, Table 5.4 provides detailed mean and standard deviation values of $SHGC_{glo}$ for each slat angle sorted based on the amount of global solar radiation. The uncertainty range ($\pm 2\sigma$) of $SHGC_{glo}$ due to environmental variables was observed to have a range between 0.008 and 0.148, depending on the slat angle. In other words, by comparing the variation of $SHGC_{glo}$ (0.05-0.52) according to the slat angle, the magnitude of uncertainty reached a maximum level of 22%. This implies that the relative superiority among slat angles can change, or the difference in values can be significantly reduced depending on the environmental conditions.

Furthermore, as mentioned earlier in Figure 5.2, the slat angle of -80° exhibited a similar average value (0.300) to that of 0° (0.277). Although it was lower than 0° within the range of global solar radiation range 350-500 W/m^2, it was higher than at 0° by 0.06 (=0.322-0.262) as the amount of global solar radiation increased, particularly in the range of 900-1,000 W/m^2. To examine specifically the cases of each slat angle, it is noticeable that as global solar radiation increases, except for slat angle at -80°, the mean value of $SHGC_{glo}$ decreases and the standard deviation increases (Table 5.4). This is because the proportion of direct radiation in global radiation increases, leading to a greater influence of $SHGC_{dir}$, which has a lower average value and higher uncertainty.

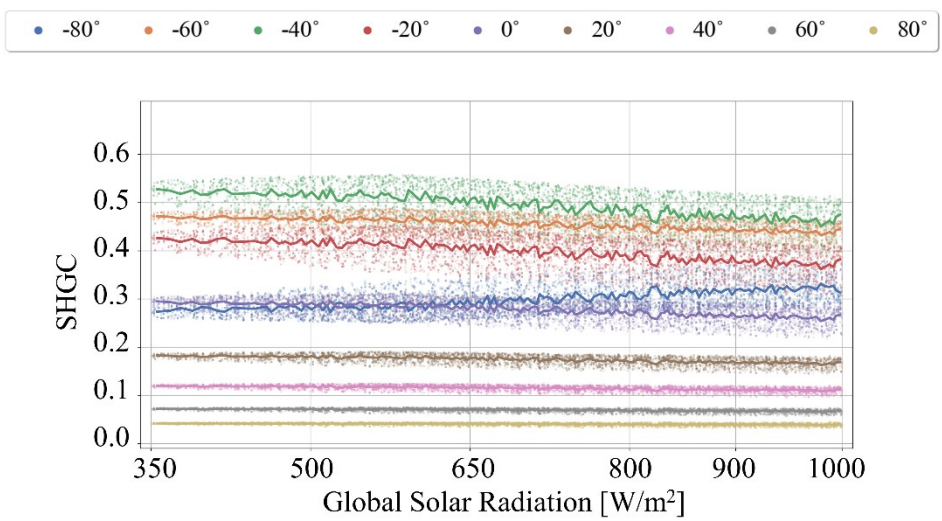

Figure 5.4 $SHGC_{glo}$ variation according to global solar radiation

Table 5.4 Mean and standard deviation of $SHGC_{glo}$ at each slat angle under varying global solar radiation

Global Radiation		Slat Angle								
		-80°	-60°	-40°	-20°	0°	20°	40°	60°	80°
350-500 [W/m^2]	μ	0.280	0.468	0.520	0.420	0.291	0.181	0.119	0.072	0.042
	σ	0.017	0.011	0.022	0.019	0.012	0.006	0.003	0.002	0.002
500-650 [W/m^2]	μ	0.286	0.464	0.512	0.413	0.287	0.179	0.118	0.071	0.041
	σ	0.024	0.016	0.032	0.027	0.017	0.008	0.005	0.003	0.002
650-800 [W/m^2]	μ	0.300	0.454	0.493	0.397	0.277	0.174	0.115	0.069	0.041
	σ	0.026	0.017	0.034	0.029	0.018	0.009	0.005	0.003	0.002
800-900 [W/m^2]	μ	0.313	0.446	0.476	0.383	0.268	0.170	0.112	0.068	0.040
	σ	0.026	0.018	0.034	0.029	0.018	0.009	0.006	0.004	0.003
900-1000 [W/m^2]	μ	0.322	0.440	0.466	0.374	0.262	0.167	0.111	0.067	0.039
	σ	0.026	0.017	0.034	0.028	0.018	0.009	0.006	0.004	0.003
total	μ	0.300	0.455	0.494	0.398	0.277	0.174	0.115	0.070	0.041
	σ	0.028	0.019	0.037	0.031	0.020	0.010	0.006	0.004	0.002

5.2 Seasonal Uncertainty Analysis

For seasonal comparison, two specific points representing typical seasons were selected: June 21st at 1 pm with a solar altitude of 73.9° and a solar azimuth of -31.6° and December 21st at 1 pm with a solar altitude of 28.6° and the solar azimuth of -8.6°. These points were chosen to evaluate the uncertainty of the system's SHGC under conditions of sufficient solar radiation. Based on the sensitivity analysis conducted previously, the three most influential environmental variables, direct solar radiation, diffuse solar radiation, and outdoor wind velocity, were selected for sampling. In order to reflect real-world conditions, instead of directly sampling the specific values of direct and diffuse solar radiation each, the ratio of global radiation to direct radiation was sampled to input to account for the cloud factor. For each month, the clearest and cloudiest days were identified, and the ratio of direct radiation to global radiation was calculated and used as the sampling range. Finally, the minimum and maximum values of these three variables were defined (Table 5.5), and a total of 2,000 samples were generated by the Latin Hypercube Sampling method.

Table 5.5 Sampling range of June and December

		Global Solar Radiation	Ratio (I_{dir} / I_{glo})	Wind Velocity
June	min	301 W/m^2	0.017	1 m/s
	max	1012 W/m^2	0.763	4.6 m/s
December	min	145 W/m^2	0.001	0.6 m/s
	max	902 W/m^2	0.919	4.6 m/s

Each point in Figure 5.5 represents a single result, the distribution of 2,000 samples for 19 different slat angles, and the line of mean values are depicted. First of all, a significant difference is observed in the range of $SHGC_{glo}$ by season. In the case of June, $SHGC_{glo}$ ranged from 0 to 0.56, while it ranged from 0 to 0.71 in December, influenced by both environmental variables and slat angles. Irrespective of the season, the uncertainty of $SHGC_{glo}$ increased when the slats rotated downward, and the uncertainty decreased when they were rotated upward, with a small deviation observed in slat angles over 30°.

Moreover, a notable difference was also observed based on the ratio of direct and diffuse solar radiation. Under clear sky conditions with a high proportion of direct solar radiation, at the slat angle closest to the solar altitude (-70° in June and -30° in December) exhibited the highest $SHGC_{glo}$, primarily influenced by $SHGC_{dir}$.

Therefore on days with clear skies, it can be inferred that the slat control angle at which the maximum $SHGC_{glo}$ is obtained will vary as the position of the sun changes throughout the day.

In contrast, under overcast sky conditions with a high proportion of diffuse solar radiation, the impact of environmental conditions on the uncertainty of $SHGC_{glo}$ is negligible, and there is no significant difference observed between the two time points. It is because, as previously found, $SHGC_{dif}$ has small uncertainty due to variations in environmental conditions and solar position. Thus, it can be inferred that on days with a high proportion of diffuse solar radiation, the $SHGC_{glo}$ will be primarily determined by the slat angle rather than the environmental conditions.

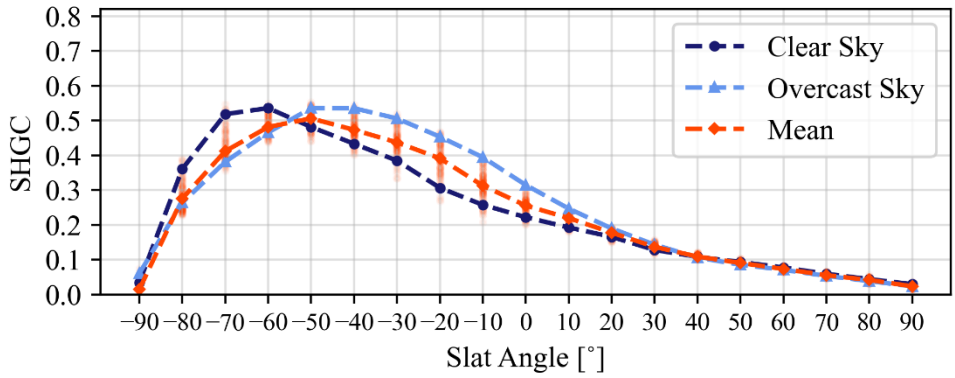

(a) June

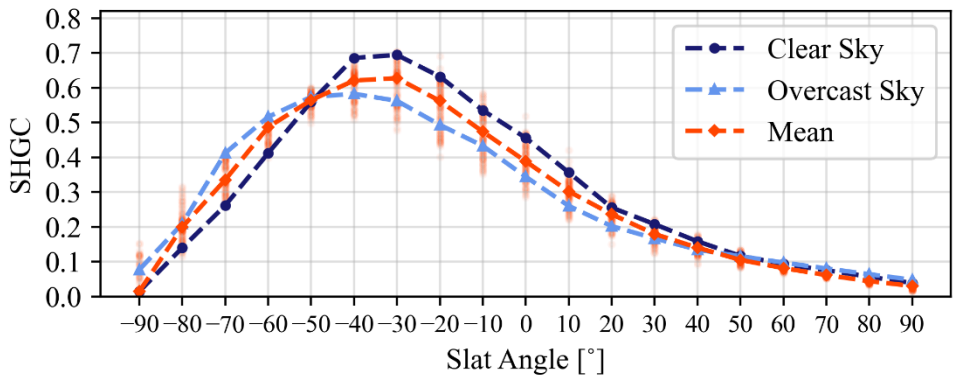

(b) December

Figure 5.5 SHGC variation in June and December

5.3 Diurnal Uncertainty Analysis

To examine SHGC variations throughout the day, the time zones between 9 am and 5 pm were analyzed at hourly intervals in summer (June, July, August) and winter (November, December, January). The sun's position for each time zone was determined based on June 21st and December 21st. The sampling ranges of the three environmental variables were defined based on weather data of Seoul and represented in Figure 5.6. 2,000 samples were generated for each time zone to conduct the uncertainty analysis.

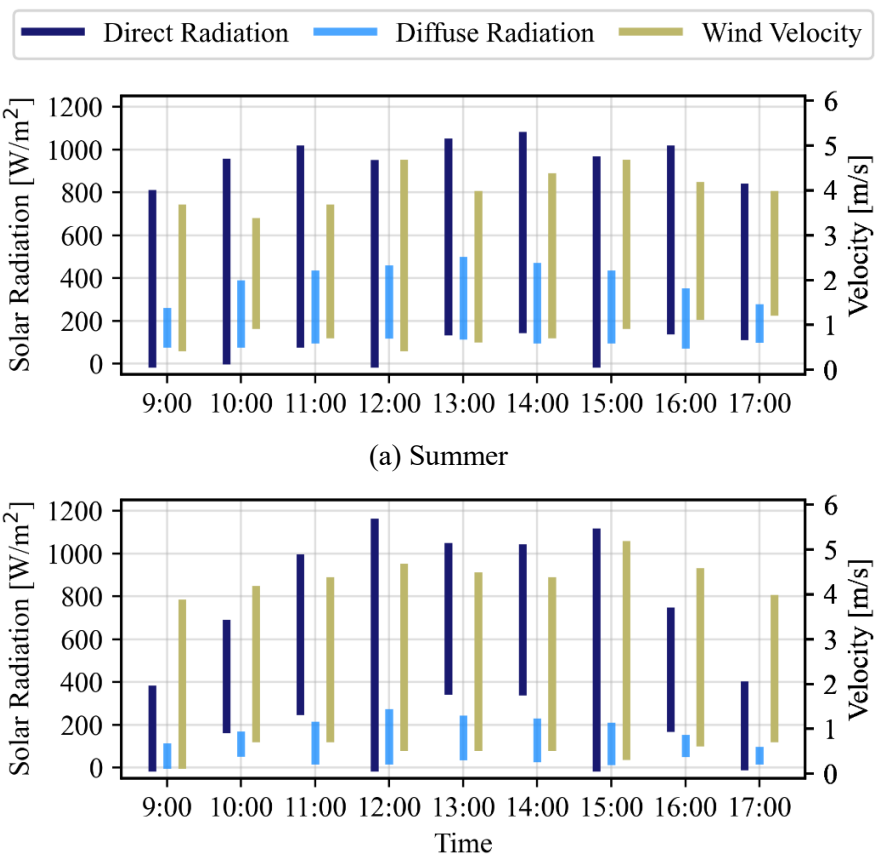

(a) Summer

(b) Winter

Figure 5.6 Sampling ranges of three variables in each time zone

Figure 5.7 illustrates the diurnal variation of mean SHGC at 19 different slat angles. Each curve represents the mean SHGC in a single time zone and, for convenience, five time zones at two-hour intervals are presented in the figures.

During the summer season , the variation in SHGC remained similar, regardless of the time of day. By examining every single line, the ranges of SHGC achievable through control of slat angle can be observed at each time zone. The range was largest at 13:00, with a minimum value of 0.02 and a maximum of 0.5. At 17:00, the range was the smallest, with a minimum value of 0.02 and a maximum value of 0.48. However, the size did not exhibit significant differences across the time zones. The maximum SHGC values were observed at slat angles of -40˚, -50˚, or -60˚, but the difference in the maximum SHGC was not substantial when comparing different time zones throughout the day (Table 5.6).

In contrast, the results obtained during the winter season differed significantly from those observed in summer. Unlike summer, the shape of the curve depicting SHGC values varied considerably over time. The maximum SHGC values were obtained at slat angles of -10˚, -20˚, or -30˚ within each time zone, with differences of up to 0.22 (=0.73-0.51). Furthermore the SHGC ranged from 0.02 to 0.72 at 13:00 and from 0.04 to 0.5 at 17:00, indicating a substantial width difference. Compared to the summer season, the thermal performance of the shading system in the winter season exhibited relatively greater variability in SHGC across different time zones throughout the day.

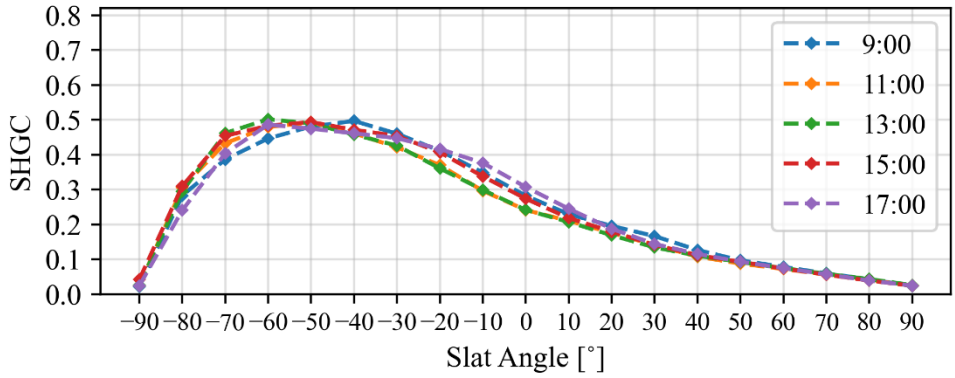

(a) Summer season

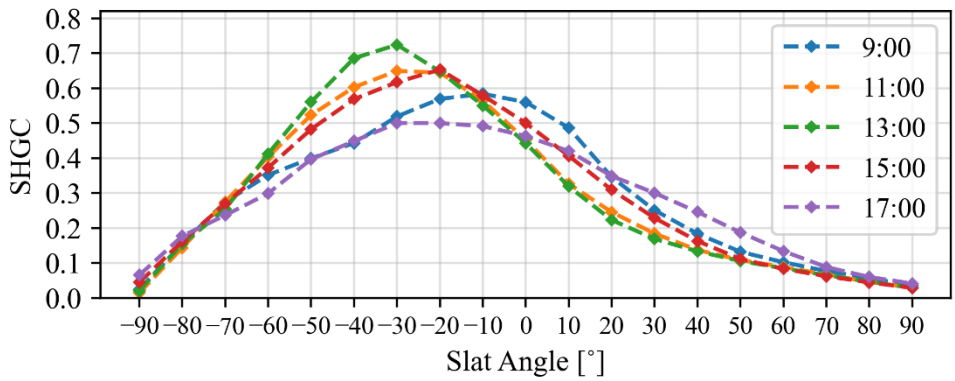

(b) Winter season

Figure 5.7 Mean SHGC by time zone

Table 5.6 Slat angle where the maximum SHGC is obtained and the SHGC

	Summer		Winter	
Time	Slat Angle	SHGC	Slat Angle	SHGC
9:00	-40˚	0.49	-10˚	0.59
10:00	-40˚	0.49	-10˚	0.63
11:00	-50˚	0.50	-30˚	0.65
12:00	-50˚	0.50	-30˚	0.67
13:00	-60˚	0.51	-30˚	0.73
14:00	-60˚	0.50	-30˚	0.71
15:00	-60˚	0.49	-20˚	0.63
16:00	-60˚	0.48	-20˚	0.61
17:00	-60˚	0.48	-20˚	0.51

The daily mean SHGC of the shading system, when the slat control angle is kept consistent throughout the day, was examined. As presented in Table 5.7, the maximum daily mean SHGC of 0.49 was observed at a slat angle of -50˚ in the summer season. While in the winter season, the maximum mean of 0.61 at slat angles of -20˚ and -30˚ was observed. Across both seasons, the daily mean SHGC decreased as the slats rotated upwards.

Table 5.7 Daily mean SHGC by slat angle

Slat Angle	Summer	Winter
-90˚	0.03	0.03
-80˚	0.29	0.15
-70˚	0.43	0.27
-60˚	0.48	0.37
-50˚	0.49	0.48
-40˚	0.47	0.57
-30˚	0.43	0.61
-20˚	0.39	0.61
-10˚	0.33	0.57
0˚	0.27	0.5
10˚	0.22	0.39
20˚	0.18	0.29
30˚	0.14	0.22
40˚	0.11	0.17
50˚	0.09	0.13
60˚	0.07	0.1
70˚	0.06	0.07
80˚	0.04	0.05
90˚	0.02	0.03

Data on the daily and hourly mean SHGC provides not only for the dynamic blind control systems but also for occupants valuable insights who can actively implement manual control strategies. They can utilize information occupants can gain an intuitive understanding of the variation of performance depending on the slat angle, and thus can establish manual control strategies of the shading system to optimize energy usage. For instance, during the summer season when it is advantageous to maintain a low SHGC for reducing cooling loads, occupants can effectively manage the shading system by adjusting the slats upward. Similarly, during the winter season, maintaining the slat angle within the range of -40˚ to -10˚ throughout the day might ensure a sufficiently high daily average SHGC leading to reduced heating loads. In other words, occupants can intuitively understand the uncertainty of SHGC of the shading system according to the slat angle and can control the system, additionally considering factors that reflect individual preferences, such as indoor illuminance and a view to outdoor.

Chapter 6. Conclusion

Solar heat gain coefficient of the shading system, obtained through physical experiments, may differ from its actual performance under dynamic environmental conditions and control methods. Therefore in the study, instead of using a physical chamber, the SHGC of the system was calculated within a virtual testbed, which incorporates the pyWinCalc module and can take into account the system's optical properties, parameterized environmental conditions, encompassing both design and control variables. The $SHGC_{glo}$ is employed as an indicator of the system's thermal performance, considering both direct and diffuse solar radiation. Environmental variables that influence SHGC were selected from physical formulas, and the pyWinCalc module was used to simulate the thermal behavior of the window system. The stochastic characteristics of the shading device's performance, considering control angles and dynamic environmental conditions.

The results of study can be summarized as follows:

- SHGC exhibits stochastic characteristics and significant uncertainty due to both dynamic environmental conditions and slat control angles. Differences in SHGC occur not only between different seasons but also at different time zones of the day.
- $SHGC_{dir}$ has relatively high uncertainty caused by dynamic environmental variables, while $SHGC_{dif}$ remains relatively constant. As a result, the average value, uncertainty, and sensitivity to environmental variables of $SHGC_{glo}$ are highly relevant to the proportion of direct and diffuse solar radiation in global solar radiation.

The findings will contribute to the development of optimal control algorithms for external Venetian blinds. Without objective quantification of the slat angle's influence on transparent building envelopes, it would lead to a significant performance gap (Augenbroe, 2019). Thus the influence of the slat angle on the thermal performance of the window as well as its corresponding uncertainty and sensitivity must be carefully reflected for assessing the thermal performance of the window system. In addition, such slat angle's influence could be beneficially applied to optimal control of dynamic shades (Kim & Park, 2012). It can be expected that this study can contribute to objectively evaluating the thermal performance of adjustable shading devices and to developing a guideline for optimal slat controls by occupants.

References

ASHRAE (2019). ASHRAE Standard 90.1-2019 – Energy Standard for Buildings Except Low-Rise Residential Buildings. Atlanta, GA, USA: American Society of Heating, Refrigerating, and Air-conditioning Engineers.

Augenbroe, G. (2019). The role of simulation in performance-based building. *Building performance simulation for design and operation* , 343-373. Spon Press, New York, USA.

Choi, Min-Seo, & Chang, Seong-Ju. (2013).Comparative Analysis on the Heating and Cooling Loads Associated with U-value, SHGC and Orientation of the Windows in Different Regions. KIEAE Journal, 13(2), 123-130.

Curcija C., Vidanovic S., Hart R., Jonsson J., Powles R. & Mitchell R. (2018). *WINDOW Technical Documentation.* Lawrence Berkeley National Laboratory. https://windows.lbl.gov/tools/window/documentation.

de Wilde, P. (2014). The Gap Between Predicted and Measured Energy Performance of Buildings: A Framework for Investigation. *Automation in Construction*, 41, 40-49.

de Wit, S., & Augenbroe, G. (2002). Analysis of uncertainty in building design evaluations and its implications. Energy and Buildings, 34(9), 951-958.

Hopfe, C. J. 2009. *Uncertainty and Sensitivity Analysis in Building Performance Simulation for Decision Support and Design Optimization*. PhD thesis, Technische Universiteit Eindhoven, Eindhoven, Netherlands.

Hopfe, C. J., & Hensen, J. L. (2011). Uncertainty analysis in building performance simulation for design support. *Energy and Buildings,* 43(10), 2798-2805.

Huchuk, B., Gunay, H. B., O'Brien, W., & Cruickshank, C. A. (2016). Model-based predictive control of office window shades. *Building Research & Information*, 44(4), 445-455.

McKay, M. D., R. J. Beckman, and W. J. Conover. 2000. "A comparison of three methods for selecting values of input variables in the analysis of output from a computer code". *Technometrics,* 42(1), 55-61.

ISO. (2003). *Thermal performance of windows, doors and shading devices - Detailed calculations* (ISO Standard No. 15099). Retrieved from https://www.iso.org/standard/26425.html.

Kim, D. W., & Park, C. S. (2010). Energy performance assessment of a double skin façade with different control strategies. *J. Archit. Inst. Korea,* 26, 389-398.

Kim, D. W., & Park, C. S. (2012). Comparative control strategies of exterior and interior blind systems. *Lighting Research & Technology,* 44(3), 291-308.

Kohler C., Mitchell R., Curcija C., Vidanovic D. & Czarnecki S. (2019). *Berkeley Lab WINDOW Calc Engine (CalcEngine) v2.* https://github.com/LBNL-ETA/pyWinCalc/tree/develop.

Kreider, J. F., Reddy, T. A., Curtiss, P. S., & Rabl, A. (2016). *Heating and cooling of buildings: principles and practice of energy efficient design.* CRC press.

KS L 9107. (2014). Testing method for the determination of solar heat gain coefficient of fenestration product using solar simulator.

LBNL(Lawrence Berkeley National Laboratory). (2016). *WINDOW,* http://windows.lbl.gov/software/window.

LBNL (Lawrence Berkeley National Laboratory). (2022). *IGSDB web application*. Retrieved from https://igsdb.lbl.gov/.

Mara, T. A., & Tarantola, S. (2008). Application of global sensitivity analysis of model output to building thermal simulations. In *Building Simulation*, 1(4), 290-302. Springer Berlin Heidelberg.

May-Ostendorp, P.T., Henze, G. P., Rajagopalan, B., & Corbin, C. D. (2012). Extraction of supervisory building control rules from model predictive control of windows in a mixed mode building. *Journal of Building Performance Simulation*, 6(3), 199–219.

NFRC (National Fenestration Rating Council). (2020). *Procedure for Determining Fenestration Product Solar Heat Gain Coefficient and Visible Transmittance at Normal Incidence* (NFRC Standard No. 200). Retrieved from http://www.nfrc.org.

Park, Yool, & Park, Jong-Il. (2010). A study of Energy use Impacts by SHGCs of Windows in Detached House. Korean Journal of Air-Conditioning and Refrigeration Engineering, 22(4), 189-196.

Saltelli, A., Ratto, M., Andres, T., Campolongo, F., Cariboni, J., Gatelli, D., & Tarantola, S. (2008). *Global sensitivity analysis: the primer*. John Wiley & Sons.

Sobol, I. M. (1993). Sensitivity analysis for non-linear mathematical models. *Mathematical modelling and computational experiment*, 1, 407-414.

국문초록

투명 외피를 통한 열전달을 조절하는 차양 장치의 정량적인 평가 지표로 SHGC가 사용되고 있고, 이는 건물 에너지 소비량 평가의 중요한 인자로 작용한다. 기존 정적 조건의 실험을 통해 구해진 차양 시스템의 SHGC는 동적으로 변화하는 환경 조건과 차양의 제어 방법에 의해 실제 성능과 차이가 있을 수 있다.

이에 따라 본 연구에서는 pyWinCalc를 이용하여 환경 변수, 슬랫 각도, 태양의 위치를 파라미터화하여 외부 베네시안 블라인드가 설치된 창호 시스템의 동적 SHGC를 별도의 건물 모델링 없이 독립적으로 분석하였다. 물리 수식으로부터 SHGC에 영향을 미치는 환경 변수를 선정하고, 전역 민감도 분석 방법을 적용하여 각 환경 변수가 SHGC에 미치는 영향을 확인하였으며 슬랫의 제어 각도에 따른 민감도의 크기와 순위가 변화함을 확인하였다. 또한, 한 시점, 계절별, 그리고 하루를 기준으로 환경 조건과 슬랫의 각도에 따른 SHGC의 확률적 특성과 불확실성을 확인하고, 변화하는 SHGC의 범위와 분포를 분석하였다.

연구를 통해 가변형 차양 시스템이 설치된 창호 시스템의 SHGC에 대한 확률적 접근의 필요성과 차양 동적 제어의 중요성을 확인하였다. 연구의 결과는 차양의 운영 단계에서 직관적인 이해를 돕는 지표가 되어, 동적 블라인드 제어뿐만 아니라 재실자의 수동 제어에서도 활용되기를 기대한다.

주요어 : 외부 베네시안 블라인드, 태양열 취득계수, 불확실성 분석, 민감도 분석, Performance gap

학 번 : 2021-26763